Compton-Profile Measurements of N_2, O_2, and Ne Using Silver and Molybdenum X-Rays

P. Eisenberger
Bell Telephone Laboratories, Murray Hill, New Jersey 07974
(Received 13 August 1971)

Compton-profile measurements have been performed on O_2, N_2, and Ne using silver and molybdenum radiation. An approach is outlined to correct for the breakdown of the impulse approximation for the 1*s* core electrons. A detailed relationship involving experimental corrections is specified by which one can relate the experimentally measured intensity to the Compton profile. Good agreement is found between the silver and molybdenum results on the long-wavelength side of the Compton profile. Comparison of the Ne experimental results both with Hartree-Fock calculations and calculations which include non-Hartree-Fock correlation effects show that within the experimental error agreement is obtained with the latter calculation. The experimental results for N_2 and O_2 are compared with theoretical calculations.

I. INTRODUCTION

In recent years there has been a resurgence in theoretical and experimental studies of Compton x-ray scattering.[1-8] A large majority of experimental work was performed using molybdenum radiation on rather complicated solid-state or molecular systems. In addition, very few experimental details were given in the various works as to how the data were analyzed and in most cases only graphic data were provided. The study of He and H_2[8] demonstrated the ability of the Compton scattering technique to measure the Compton profile (CP) with a high degree of accuracy for those simple systems. Theoretical work[7] on the problems of studying electronic systems in which the electrons are strongly bound indicated that corrections were required to the simple impulse approximation (IA) in order to obtain accurate information about the CP. These corrections were shown to be more serious the smaller the recoil energy transferred to electrons in the Compton process, and consequently depend upon the energy and scattering angle used in the experimental investigations. The experimental corrections, absorption, dispersion, and detection efficiency are also more serious in the systems with tightly bound electrons because the CP is spread over a much larger-wavelength region. In the simpler systems such as He and H_2, the experimental corrections could be ignored because of the extreme narrowness of their CP. However, for the systems of interest in this study, the corrections are no longer negligible and must be taken into account. These corrections also depend upon the radiation used to measure the CP.

The experimental results for Ne, N_2, and O_2 and their comparison with theoretical calculations have been previously published.[3] In this work, we will concentrate on the experimental details and give an extended discussion of the results. All systems were studied with both silver and molybdenum radiation. Corrections to the IA for 1*s* core electrons in those systems will be applied. The quantitative comparison between the silver and molybdenum results show that the procedure for reducing the data which is outlined in this paper produces consistent experimental results.

In Sec. II of this paper we briefly review the theory of Compton x-ray scattering and outline the approach used to make the corrections to the IA. In Sec. III the experiment is discussed and the procedure used to analyze the data is presented. In Sec. IV the experimental results are given and are compared with theoretical calculations.

II. BASIC THEORY

As previously described[6,7] the free-electron theory of Compton scattering when applied to weakly bound electrons is called the IA. From those works the cross section in the IA is given by

$$\frac{d\sigma}{d\omega d\Omega} = \left(\frac{d\sigma}{d\Omega}\right)_{\mathrm{Th}} \frac{\omega_1}{\omega_2}\left(\frac{1}{2\pi}\right)^3 \int n(\vec{p}_0)d^3p_0 \times \delta\left(\omega - \frac{k^2}{2m} - \frac{\vec{k}\cdot\vec{p}_0}{m}\right), \quad (1)$$

where $(d\sigma/d\Omega)_{\mathrm{Th}}$ is the Thompson cross section, ω_1 and ω_2 are the initial and final energies of the photon ($\hbar = 1$), $\omega = \omega_1 - \omega_2$, and $\vec{k} = \vec{k}_1 - \vec{k}_2$ is the momentum transfer to the system where $\vec{k}_1$ and $\vec{k}_2$ are the initial and final photon momenta. The quantity $n(\vec{p}_0)$ is the probability of the electrons having momentum $\vec{p}_0$. For isotropic systems or spherically averaged systems Eq. (1) can be rewritten to take the form

$$\left(\frac{d\sigma}{d\omega\, d\Omega}\right) = \left(\frac{d\sigma}{d\Omega}\right)_{\mathrm{Th}} \frac{\omega_1}{\omega_2}\frac{m}{|k|} J(q), \quad (2)$$

where the CP, $J(q)$, is given by

$$J(q) = 2\pi \int_q^\infty n(p_0) p_0 \, dp_0 \tag{3}$$

and where q is the projection of the electron's momentum on the scattering vector $\vec{k}$:

$$q = \vec{k} \cdot \vec{p}_0 / |k| \, . \tag{4}$$

The usual experimental approach is to study the variation of the intensity of scattering as a function of the energy of the scattered photon at a fixed angle of scattering with the characteristic radiation from an x-ray tube used as the input beam. By use of Eqs. (1) and (2) the compton profile $J(q)$ is found from the scattered intensity with the energy δ function in Eq. (1) providing the relationship between ω and q.

In this work the above described approach will be used to evaluate the CP for all the electrons except the 1s core electrons. For those electrons significant deviations from the IA are expected.

It has been shown[7] that for a 1s hydrogenic electron in which the binding of the electron is explicitly considered the cross section for Compton scattering is given by

$$\left(\frac{d\sigma}{d\Omega \, d\omega}\right) = \left(\frac{d\sigma}{d\Omega}\right)_{\mathrm{Th}} \frac{\omega_1}{\omega_2} \left\{ \frac{\pi^2 8^3 a^2}{p} (1 - e^{-2\pi/pa})^{-1} \exp\left[\frac{-2}{pa} \tan^{-1}\left(\frac{2pa}{1 + k^2a^2 - p^2a^2}\right)\right] \right.$$
$$\left. \times [k^4a^4 + \tfrac{1}{3}k^2a^2(1 + p^2a^2)] \, [(k^2a^2 + 1 - p^2a^2)^2 + 4p^2a^2]^{-3} \, \delta(E_f - E_i - \omega) \right\} , \tag{5}$$

where $1/a = Zme^2/\hbar^2$, Z is the nuclear charge, and where $p^2/2m$ is the recoil energy of the electron and at each ω the appropriate value of p is determined from the energy conservation condition

$$p^2/2m = -(E_B) + \omega \, , \tag{6}$$

where E_B is the binding energy of the 1s electron. In this work the orbital energy determined by Clementi[9] for the 1s electrons in his Hartree-Fock calculations is used for E_B and by use of the simple relationship for energy of a 1s hydrogenic electron an effective Z, Z_{eff} is calculated. The value of Z_{eff} found is used to calculate the value of a in Eq. (5). Equation (5) is then used to evaluate the contribution to Compton scattering by the 1s core electrons. By comparing Eq. (1) and (5) at each wavelength or value of q the magnitude of the corrections to IA are determined.

In the experiments reported here the angle between the incident and scattered photon was fixed at 170° but the magnitude of k^2 was roughly a factor of 1.5 larger for the silver experiments than the molybdenum experiments because of the higher energy of the silver characteristic radiation (22.163 keV compared to 17.374 keV). In Table I are listed the ratios of the results calculated on the basis of Eq. (5) to that calculated by the IA for values $q = 0$ to $q = 10$, the long-wavelength side of the Compton profile, under the experimental conditions just described for both silver and molybdenum studies of N_2, O_2, and Ne.

The correction procedure described above is only exact for the case of a hydrogenic atom. For a many-electron atom a correct treatment would allow for the readjustment of charge at the atomic site following the removal of the recoiling electron. The solution of that problem is quite difficult and no simple analytical result exists. However, except near the threshold when the recoil energy is equal to the binding energy of the electron, one would not expect the many electron features to play a major role.

III. EXPERIMENT

The experimental configuration is shown in Fig. 1. It is the same as shown previously[8] except that the pressure cell is included. The experimental apparatus and procedure for data taking was identical to that described previously except for the addition of a $K\beta$ filter on the input x-ray beam when silver radiation was used. The filter was required in those experiments because the tightly bound electrons in N_2, O_2, and Ne systems Compton scatter over such a broad energy range that the scattering caused by the $K\beta$ characteristic lines overlaps that caused by the $K\alpha$ characteristic lines.

TABLE I. Ratio of the Compton profile as determined by Eq. (5) to that determined by the IA, Eq. (2), for the 1s electrons in N_2, O_2, and Ne when silver and molybdenum radiation are used at a scattering angle of 170°.

	N_2		O_2		Ne	
q	Ag	Mo	Ag	Mo	Ag	Mo
0	0.965	0.943	0.953	0.925	0.925	0.880
1	0.937	0.913	0.926	0.897	0.902	0.860
2	0.926	0.902	0.914	0.886	0.889	0.852
3	0.933	0.913	0.917	0.893	0.888	0.855
4	0.957	0.943	0.934	0.916	0.898	0.871
5	0.996	0.990	0.965	0.954	0.918	0.897
6	1.046	1.051	1.007	1.005	0.948	0.934
7	1.107	1.124	1.059	1.067	0.986	0.981
8	1.176	1.207	1.119	1.139	1.032	1.036
9	1.254	1.299	1.187	1.220	1.085	1.099
10	1.338	1.400	1.261	1.309	1.144	1.170

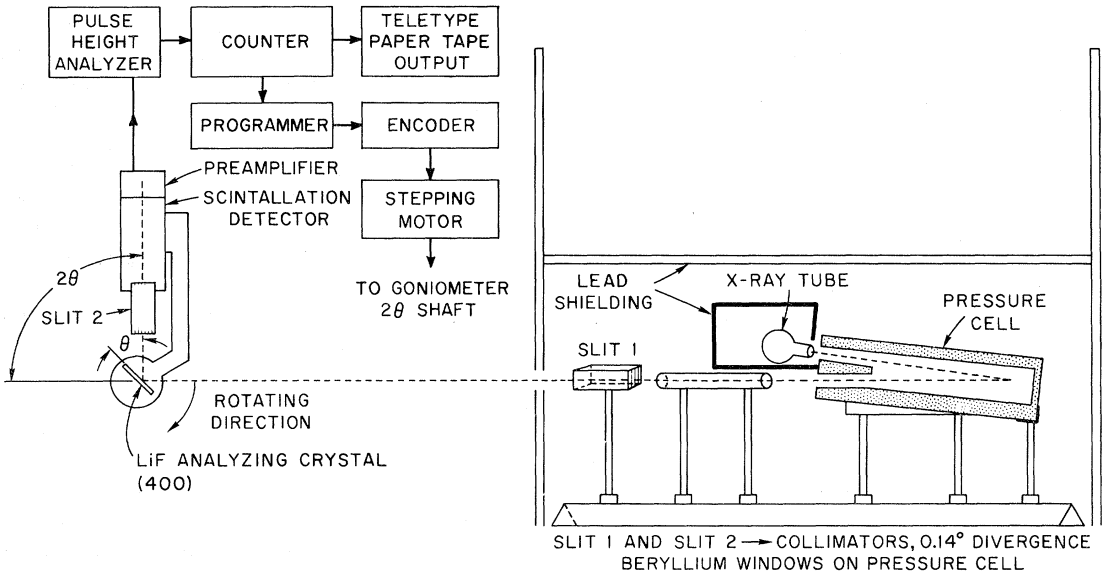

FIG. 1. Experimental apparatus. The windows on the pressure cell are $\frac{1}{8}$-in. beryllium and the scattering angle is 170°.

The pressures at which the gases were studied were adjusted so that, independent of the gas being investigated or the radiation used, the absorption of the x rays by the gas was approximately constant. The values for the pressures in lb/in.^{2} were for the silver and molybdenum experiments, respectively, as follows: N_2 (300, 535), O_2 (200, 325), and Ne (175, 250).

Figure 2 shows a typical experimental result for the systems being studied. The particular spectrum shown is of N_2 using silver radiation. The plot is the total number of counts as a function of the angular setting of the LiF analyzing crystal. It is clearly seen that there is a sloping background underneath the Compton spectrum. Pulse height analysis of the scattered spectrum gave information

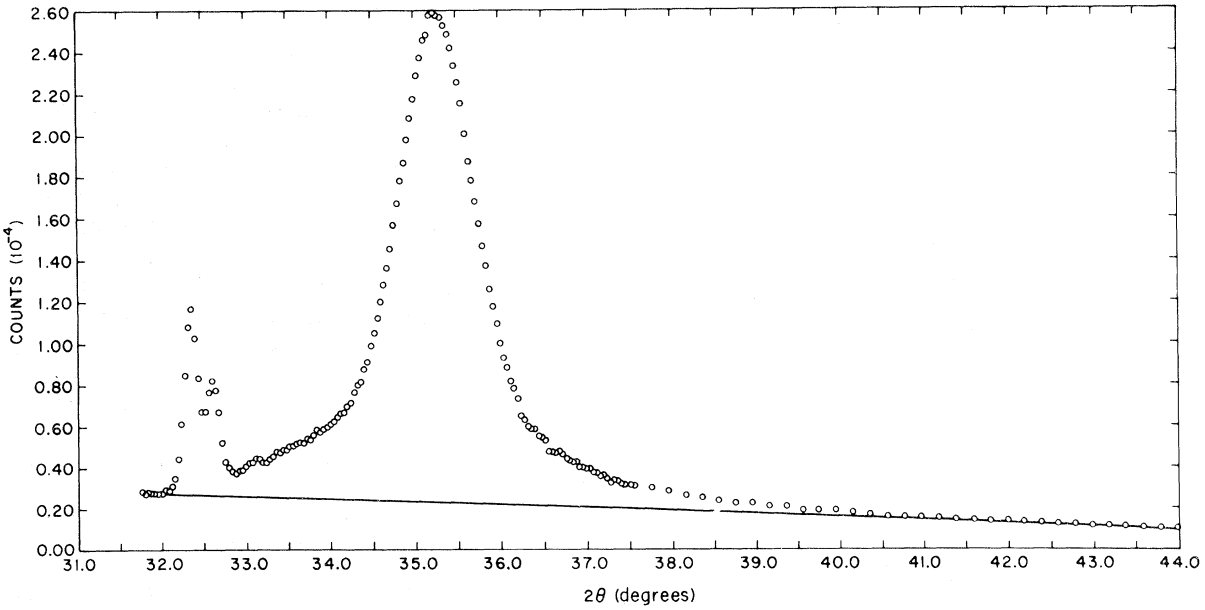

FIG. 2. Experimental results for N_2 using silver radiation. The intensity in counts is plotted as a function of the scattering angle $2\theta_B$ of the LiF analyzing crystal. As indicated, the main peak was taken in steps of 0.04° while the long tail was taken in steps of 0.2°.

about the sloping background. The output from the NaI scintillator was fed into a multichannel analyzer where the contributions from the three reflecting orders of LiF [(200), (400) and (600)] were clearly discernible. In the experiments, the LiF crystal was set for (400) scattering of the radiation which is responsible for the Compton peak; however, (200) scattering of $\frac{1}{2}$ the energy and (600) scattering of $\frac{3}{2}$ the energy was also present. It was found that in all cases the (600) scattering of $\frac{3}{2}$ the energy was the dominant component of the background on the high-wavelength side of the spectrum and moreover to a high degree of accuracy its intensity decreased linearly as one moved towards larger angles. This linear decrease over the range of LiF angles of interest in the Compton studies held for the total background in the gases and for both silver and molybdenum experiments. The rate of the linear decrease did, however, vary from one experiment to another. The above only remained true as long as one adjusted the window on the single channel pulse height analyzer used in taking the data to include all three orders of LiF scattering for all angles studied. This procedure was followed in the experiments reported in this work. Because of the long tails associated with the tightly bound 1s electrons it is very difficult to accurately choose the base line. The final procedure used will be described shortly. At this stage of the data analysis a best guess is made for the base line. For the silver experiment on N_2, N_2 (Ag), the line chosen is shown in Fig. 2.

With the linear background removed the data is curve fit in various sections to functions of the form

$$F(\theta)=\frac{A+B\theta^2+C\theta^4+D\theta^6}{1+E\theta^8+F\theta^3+G\theta^5+H\theta^7}\ . \tag{7}$$

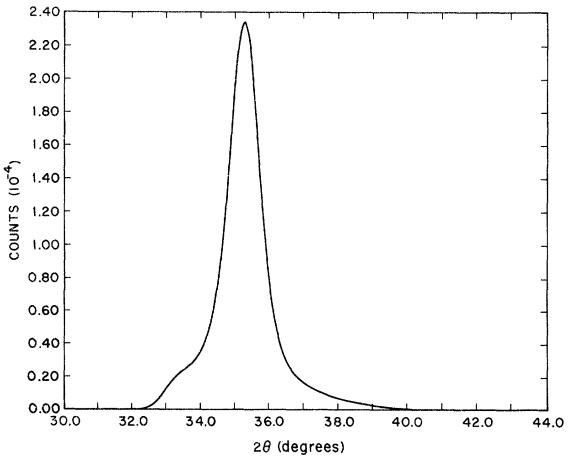

FIG. 3. Curve-fit data for N_2 using silver radiation with the background and characteristic lines subtracted. Again the intensity in counts is plotted as a function of the scattering angle $2\theta_B$ of the LiF analyzing crystal.

For N_2 (Ag), the curve-fit data are shown in Fig. 3. Note that the $K\alpha_1$ and $K\alpha_2$ photon peaks have been removed for ease in further data processing. A standard Fourier-transform technique[10] is then used to both remove the $K\alpha_2$ contribution to the scattering peak and to correct for the effects of finite resolution. Both of these effects have been previously discussed elsewhere.[8] For these broader CP the resolution effects are smaller then they were in He and H_2.

Having labeled the resulting curve $I_m(\lambda)$, where the relationship between wavelength λ and the LiF scattering angle is provided by Bragg's law, it remains to relate $I_m(\lambda)$ to $J(q)$. To do this several experimental factors must be considered. Of prime importance is a true understanding of the nature of operation of the LiF analyzing crystal. The LiF crystal takes the broad spectral width but relatively highly colliminated Compton scattered beam and by Bragg reflection analyzes the beam's spectral composition. It can be shown[11,12] that under conditions of broad spectral width and high angular collimination a Bragg scattering process in the absence of extinction reflects an input beam $I(\lambda)$ according to

$$I_m(\lambda)=\frac{I(\lambda)r_0^2n^2|F|^2\lambda^4(1+\cos^2 2\theta_B)}{8u_{\mathrm{LiF}}\sin^2\theta_B}, \tag{8}$$

where $I(\lambda)$ is the input power per unit wavelength at wavelength (λ) and $r_0=e^2/mc^2$ is the classical electron radius, n is the number of scatters per unit volume, $|F|^2$ is the appropriate structure factor for (400) LiF, u_{LiF} is the linear absorption constant, θ_B is defined by the Bragg relationship, $\lambda=2d\sin\theta_B$ with d the spacing of the (400) planes in LiF. In deriving Eq. (8), it was assumed that when the LiF crystal was set at a position to reflect λ_0 that $I(\lambda)$ varied slowly in the region of λ_0 compared to variation of the efficiency of reflection in the region of λ_0. The above is equivalent to the statement that the effects of finite resolution are small. Besides the LiF crystal efficiency, the absorption of the scattered beam by the gas must be accounted for. It causes a reduction in the intensity of the scattered beam according to $\exp(-u_g l)$ when u_g is the wavelength-dependent linear absorption constant of the gas at the pressure it was studied and l is the path length and beam must travel to get out of the cell. Absorption effects of the $\frac{1}{8}$-in.-thick Be windows are accounted for in a similar way.

The relationship of $I(\lambda)$ in Eq. (8) to the cross-section formula in Eq. (2) is given by

$$I(\lambda)=I_{\mathrm{in}}\frac{d\sigma}{d\lambda\,d\Omega}\,\Omega_{\mathrm{out}}=I_{\mathrm{in}}\frac{d\sigma}{d\omega\,d\Omega}\,\frac{d\omega}{d\lambda}\,\Omega_{\mathrm{out}}, \tag{9}$$

where I_{in} is the input intensity and Ω_{out} is output solid angle which is determined by slit 1. Com-

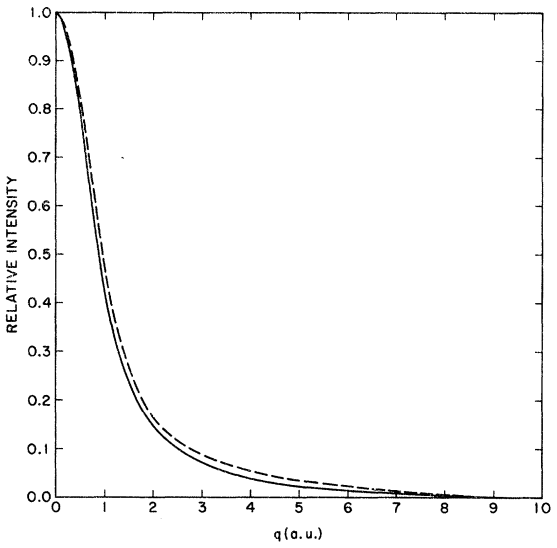

FIG. 4. Solid line is the long-wavelength side of the CP for N_2 using silver radiation after the $K\alpha_2$ contribution has been removed and the resolution corrections performed. The dotted line is the result of multiplying the solid line by the correction function $C(\theta_B, g)$.

bining all these factors one finds that

$$I_m(\lambda_2) = I(\lambda_2) e^{-(u_g l + u_{Be} t)}$$

$$= \frac{C(1+\cos^2 2\theta_B)\omega_2^2 \lambda_2^4 e^{-(u_g l + u_{Be} t)}}{u_{LiF}\lambda_2 \sin^2\theta_B k} J'(q), \qquad (10)$$

where u_{Be} is linear absorption constant for beryllium, t the thickness of the windows, and the constant C includes all the wavelength-independent factors. The absolute magnitude C is unimportant because of the previously described[8] relative nature of the Compton measurement. Note that a prime has been placed on $J(q)$ to indicate that a correction is still required to accurately fix the base line. Making use of the Bragg relationship and the approximate λ^3 dependence of the absorption constant of LiF, one finds

$$J'(q) = \frac{I_m(\lambda_2)\sin^3\theta_B(\lambda_1 + 2d\sin\theta_B) e^{(u_g d + u_{Be} t)}}{(1+\cos^2 2\theta_B)}$$

$$= I_m(\lambda_2) C(\theta_B) . \qquad (11)$$

In Eq. (11) the approximation $kc = (\omega_1 + \omega_2)$ was made which for a 170° scattering angle is accurate to better than 1%.

In Fig. 4 $I_m(\lambda_2)$ is plotted for N_2 using Ag radiation on the long-wavelength side of the Compton peak and also the result of Eq. (11). The relationship between q and λ is provided by the energy δ function in Eq. (1). Significant changes are seen to result from the experimental corrections. We are emphasizing the long-wavelength side of the Compton profile because in the final analysis it is that region which will be used to compare theory and experiment so as to minimize problems with the impulse approximation for the outer electrons.

At this stage in the data analysis a check is made of the accuracy of the initial background subtraction. This is done by comparing the theory and experimental results for $J(q)$ in the region $q = 7-10$ under the condition that the area under the two curves $q = 0-10$ are the same. In that region the $1s$ core electrons dominate the intensity. For the comparison results from the impulse corrected theory were used. Calling the difference between the theory and experiment in the region $q = 7-10$ $D(q, \theta_B)$, the function $D(q, \theta_B)\, C(\theta_B)$ was then plotted to check if it was a straight line as expected if the difference resulted from the wrong choice of the background. In all cases the function was found to be a straight line and, for example, the correction appropriate for the nitrogen data shown in Figs. 2–5 was $-1.3 \times 10^{-2} + 1.4 \times 10^{-3} q$. The functional form of $D(q,\theta_B)/C(\theta_B)$ was used to determine the appropriate corrections in the region $q = 0-7$.

After applying the correction, the data were scaled by use of the previously given normalization condition

$$\int_{-\infty}^{\infty} J(q)\, dq = 1/\text{electron} \qquad (12)$$

for the valence electrons and using the impulse corrected theory to determine the $1s$-core-electrons contribution to the area.

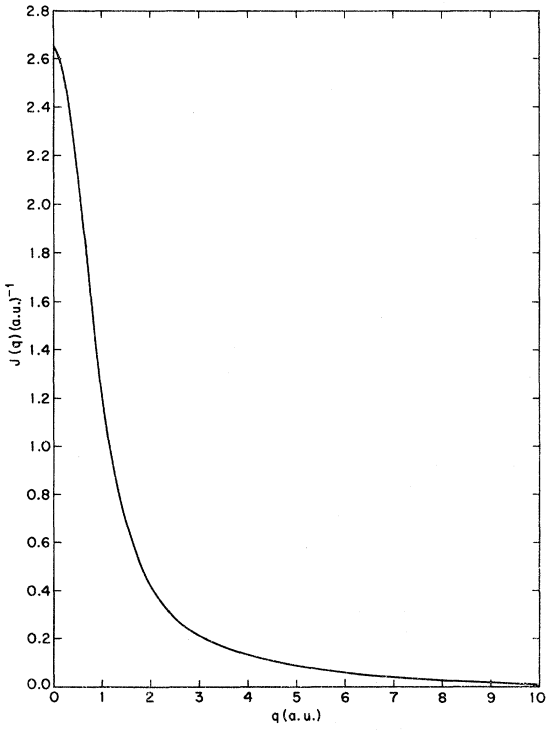

FIG. 5. Final results for the Compton profile of N_2.

TABLE II. Experimental values for the Compton profile $J(q)$ for N_2, O_2, and Ne with the 1s core contribution subtracted out. For N_2 and O_2 the Compton profile is normalized to 5 and 6 electrons, respectively. Also included are results for helium gas.

	N_2		O_2		Ne		He	
q	Ag	Mo	Ag	Mo	Ag	Mo	Ag	Mo
0	2.419	2.387	2.435	2.429	2.565	2.598	1.065	1.066
0.1	2.392	2.364	2.423	2.416	2.556	2.592	1.056	1.052
0.2	2.319	2.303	2.382	2.375	2.536	2.577	1.022	1.012
0.3	2.207	2.198	2.311	2.302	2.505	2.533	0.964	0.954
0.4	2.061	2.055	2.213	2.195	2.438	2.465	0.887	0.876
0.5	1.887	1.887	2.088	2.064	2.350	2.369	0.797	0.789
0.6	1.699	1.706	1.941	1.914	2.243	2.255	0.701	0.700
0.7	1.504	1.517	1.777	1.751	2.122	2.126	0.606	0.612
0.8	1.317	1.339	1.602	1.584	1.988	1.984	0.516	0.527
0.9	1.141	1.172	1.426	1.420	1.842	1.836	0.437	0.448
1.0	0.981	1.011	1.252	1.264	1.690	1.679	0.369	0.382
1.2	0.718	0.746	0.947	0.974	1.398	1.390	0.267	0.275
1.4	0.527	0.547	0.715	0.752	1.134	1.145	0.197	0.195
1.6	0.391	0.405	0.551	0.567	0.912	0.930	0.143	0.137
1.8	0.290	0.293	0.429	0.420	0.744	0.754	0.101	0.098
2.0	0.205	0.224	0.328	0.321	0.611	0.605	0.072	0.067
2.5	0.093	0.107	0.175	0.177	0.366	0.347	0.037	0.027
3.0	0.046	0.054	0.117	0.115	0.228	0.222	0.018	0.008
3.5	0.034	0.027	0.065	0.076	0.154	0.158	...	...
4.0	0.027	0.019	0.030	0.028	0.094	0.111	...	...
5.0	0.012	0.010	0.017	0.011	0.047	0.036	...	...

The effect of $C(\theta_B)$ on the data is much greater than the base-line correction, which, under the constant area restriction, resulted in less than 1% corrections to the Compton peak. Further discussion of the effect of experimental corrections on the accuracy of the final results is deferred until Sec. IV, in which the experimental results are presented.

Even though only results for the long-wavelength side of the Compton profile will be given in this work, the short-wavelength side in the region $q = 0-2$ was checked in each experiment to see if the asymmetry expected from impulse-type corrections was observed. In all cases the expected asymmetry was observed. In Ne(Mo) the 1s core electrons which have an 887-eV binding energy[9] cannot contribute to the CP at $q = -2$ and thus a larger asymmetry (20%) was expected and was, in fact, observed.

In general the asymmetry is, of course, fairly sensitive to the choice of $q = 0$ which is in the IA solely determined by the energy δ function in Eq. (2). Experimentally, the LiF crystal was calibrated before and after each run to check the relationship between the angular scale on the diffractometer and the wavelength. The accuracy of that calibration caused an uncertainty in $q = 0$ of $\pm$ 0.02 a.u. or about $\frac{1}{10}$ of the resolution half-width of the system.

Finally it should be noted that as shown in Fig. 2 the edges due to the 1s core electrons in N_2 and O_2 were observed.

IV. EXPERIMENTAL RESULTS

In Table II the results for N_2, O_2, and Ne are given for both silver and molybdenum radiation after the contributions of the impulse-corrected 1s core electrons have been subtracted. As one can see, the agreement between the silver and molybdenum results are quite good which strongly suggests that the IA is valid for the 2s and 2p electrons in those systems on the long-wavelength side of the Compton profile. Apart from systematic effects which will be discussed shortly, the agreement also indicates that the form of the experimental corrections is correct. For completeness, we have also included in Table II the results for helium gas using silver and molybdenum radiation.

In Table III are given the theoretical Compton profile[13] for Ne calculated from Clementi[9] wave functions and also a calculation by W. H. Hennecker[14] in which an attempt was made to include non-Hartree-Fock correlation effects. For comparison, the average of the silver and molybdenum experimental results is also given in Table III. The errors shown just represent the statistical uncertainty. The experimental results are seen to agree better with the correlated results than with the pure Hartree-Fock calculations based on Clementi wave functions.

A comparison of the noncorrelated, correlated, and experimental results would suggest that larger correlation effects would produce even better agreement between the theory and the experiment. This

TABLE III. Comparison between the average of the silver and molybdenum experimental results for Ne with calculations (Ref. 13) based on Clementi wave functions (Ref. 9) [Hartree-Fock self-consistent field (HF-SCF)] and calculations performed by Hennecker (Ref. 14) using wave functions in which non-Hartree-Fock correlations have been included [multiconfiguration self-consistent field (MC-SCF)].

q	Ne (HF-SCF)	Ne expt.	Ne (MC-SCF)
0	2.548	2.582	2.565
0.1	2.540	2.574	2.557
0.2	2.515	2.558	2.533
0.3	2.475	2.519	2.491
0.4	2.418	2.451	2.429
0.5	2.335	2.359	2.347
0.6	2.236	2.249	2.246
0.7	2.120	2.124	2.127
0.8	1.990	1.986	1.996
0.9	1.855	1.839	1.856
1.0	1.715	1.685	1.712
1.2	1.435	1.394	1.429
1.4	1.171	1.140	1.170
1.6	0.953	0.921	0.947
1.8	0.766	0.749	0.761
2.0	0.619	0.608	0.610
2.5	0.355	0.355	0.355
3.0	0.212	0.225	0.212
3.5	0.132	0.156	0.132
4.0	0.085	0.102	0.085
5.0	0.040	0.041	0.039

TABLE IV. Comparison between the average of the silver and molybdenum experiments for O_2 and N_2 with the results calculated from Clement (Ref. 9) wave functions for N and O atoms. The 1s core has been subtracted from both and the experimentsl results have been normalized to 5 electrons for N_2 and 6 electrons for O_2 in order to facilitate the comparison with the atomic results.

q	N_2 expt.	N theor.	O_2 expt.	O theor.
0	2.403±1%	2.536	2.432±1%	2.548
0.1	2.378	2.512	2.419	2.532
0.2	2.311	2.438	2.378	2.484
0.3	2.203	2.319	2.307	2.404
0.4	2.058	2.160	2.204	2.290
0.5	1.887	1.969	2.076	2.148
0.6	1.703	1.761	1.927	1.995
0.7	1.510	1.547	1.764	1.806
0.8	1.328	1.338	1.593	1.622
0.9	1.156	1.143	1.432	1.440
1.0	0.996±2%	0.967	1.258±2%	1.216
1.2	0.732	0.680	0.960	0.959
1.4	0.537	0.474	0.733	0.714
1.6	0.398	0.331	0.560	0.543
1.8	0.291	0.235	0.424	0.392
2.0	0.215±6%	0.170	0.324±6%	0.293
2.5	0.100	0.083	0.176	0.150
3.0	0.050±10%	0.047	0.116±10%	0.084
3.5	0.030	0.029	0.070	0.051
4.0	0.023	0.019	0.029	0.033
5.0	0.011	0.010	0.014	0.015

is, in fact, expected since the correlated calculation only accounted for 60% of the correlation energy.

In Table IV are given the average of the experimental results for N_2 and O_2 with the impulse corrected 1s core electron's contribution subtracted and the CP normalized to $\frac{1}{2}$ per electron. The Compton profile calculated[13] from Clementi wave functions[9] for atomic nitrogen and oxygen is also given in Table IV for comparison.

The first-order effect of molecular binding on the 2p electrons in N_2 and O_2 is to increase their spacial localization. In momentum space, this is equivalent to increasing the amount of high-momentum components and thus creating a broader, flatter Compton profile. As seen from Table IV, the experimentally observed CP for the molecule is broader and flatter than the CP calculated for the atomic systems. Calculations[3,15] for molecular nitrogen and oxygen have been performed in which Hartree-Fock accuracy was achieved. Those results agree much better with the experimental results than the atomic calculations. As previously pointed out,[3] the comparison of the experimental results with theoretical calculations which utilize different approximations resulted in the conclusion that extreme care must be exercised in relying on molecular calculations which have not achieved Hartree-Fock accuracy. A comparison of Table IV of this paper with Table I of Ref. 3 quantitatively shows that the *atomic* calculations for N_2 and O_2 are almost as accurate as the approximate *molecular* calculations. More details concerning the various theoretical calculations can be found in Ref. 15. Cooper and Williams[16] have recently reported some measurements on liquid nitrogen in which the deviation from atomic calculations is also observed. However, no quantitative results were given so a comparison with this work is impossible. In addition, no impulse corrections were made for the 1s electrons.

The determination of the magnitude of nonstatistical uncertainties is very difficult. Possible sources of error lie in the impulse treatment of the 1s core electrons, resolution corrections, the variation of $C(\theta_B)$, and the background subtraction. The first two are thought to be small in this work and should not make a sizable contribution to the uncertainty. If the LiF crystal was not reflecting as a perfect mosaic crystal as assumed in the calculations, then the $C(\theta_B)$ would be changed considerably which as illustrated in Fig. 4 would result in a change in the Compton profile. Experimental tests as to the nature of the reflection of the LiF analyzing crystal strongly suggest that it is, to a good approximation, reflecting as a perfect mosaic crystal. A background subtraction is always difficult and in this case the difficulty is increased by the inability to measure a background without the presence of the Compton peak.

All the above effects except the resolution correction will be largest in the tails of the Compton profile and thus should have their major effects on the experimental results in the region $q = 2.5-5$. For example, at $q = 4$ in nitrogen the 2s and 2p electrons only contribute about 4% of the measured intensity, the other 96% coming from the sloping background and the 1s electrons. Thus a 4% error in the subtraction of the background and the 1s contribution would result in a 100% error in the measured core-subtracted CP. The errors in the tail of the CP only effect the over-all curve if the error introduced is systematic (too high or too low as opposed to a random uncertainty). For example, in N_2 and O_2 there is some indication that the experimental values in the region $q = 2.5-5$ are too high. This would cause the values in the region $q = 0-2.5$ to be too small because of the constant area restriction imposed by the normalization conditions. For some cases then it might prove useful when comparing the experimental results with theoretical calculations to fit the two at $q = 0$ and then compare the variation away from $q = 0$.

At the present time, however, any further evaluation of possible systematic experimental errors

is prohibited by the lack of accurate theoretical Compton profiles. Judging from the work on neon, however, it would seem that the CP measurements presently offer a real testing ground for molecular and solid state wavefunctions. From the comparisons with theory already made for N_2 and O_2,[3] it would seem that the Compton profile could become a testing ground for the various approximate schemes used to calculate complex many-electron systems. Towards this end, work is already in progress to test various approximate schemes including the bond-additivity concept for hydrocarbons.

The experimental and computational help of W. Marra is most gratefully acknowledged. P. M. Platzman's helpful comments on the manuscript are also acknowledged. Constructive suggestions by L. Mendelsohn are greatly appreciated.

[1]W. Phillips and R. J. Weiss, Phys. Rev. 171, 790 (1968).
[2]M. Cooper and J. A. Leake, Phil. Mag. 15, 1201 (1967).
[3]P. Eisenberger, W. H. Henneker, and P. E. Cade, J. Chem. Phys. (to be published).
[4]Tomoe Fukamachi and Sukeaki Hosaya, J. Phys. Soc. Japan 29, 736 (1970).
[5]W. C. Phillips and R. J. Weiss, Phys. Rev. 182, 923 (1969).
[6]P. M. Platzman and N. Tzoar, Phys. Rev. 139, 410 (1965).
[7]P. Eisenberger and P. M. Platzman, Phys. Rev. A 2, 415 (1970).
[8]P. Eisenberger, Phys. Rev. A 2, 1678 (1970).
[9]E. Clementi, IBM J. Res. Develop. Suppl. 9, 2 (1965).
[10]A. R. Stokes, Proc. Phys. Soc. (London) 61, 382.
[11]B. E. Warren, *X-Ray Diffraction* (Addison-Wesley, Reading, Mass., 1969), pp. 54, 33.
[12]R. W. James, *The Optical Principles of the Diffraction of X-Rays* (Cornell U. P., Ithaca, New York, 1965), p. 34.
[13]R. J. Weiss, A. Harvey, and W. C. Phillips, Phil. Mag. 17, 241 (1968).
[14]W. H. Henneker (private communication).
[15]P. E. Cade and W. H. Henneker (private communication).
[16]M. Cooper and B. Williams, Phil. Mag. 22, 543 (1970).

PHYSICAL REVIEW A VOLUME 5, NUMBER 2 FEBRUARY 1972

Electron Drift in Gaseous He: Density, Temperature, and Field Dependences*

John P. Hernandez
Physics Department, University of North Carolina, Chapel Hill, North Carolina 27514
(Received 23 September 1971)

The theory of Eggarter and Cohen for the mobility edge of electrons in dense helium gas is used to perform calculations. The experimental low-field mobility is reproduced over its five-order-of-magnitude range as a function of gas density. The recently measured temperature dependence (4–20 °K) is also obtained. The low-field Hall mobility is calculated. Finally, modifications are introduced to yield the electric field dependence of the drift velocity, which is also found to be in good agreement with the experimental measurements.

The recent theoretical work of Eggarter and Cohen[1] (EC) is used to calculate the drift velocity of electrons in dense helium gas, in the neighborhood of the mobility edge. The purpose of this paper is to show that, within the context of the EC theory, it is possible to account for the drift velocity of electrons over a substantial helium density range, as EC have already shown, and also over a substantial temperature range. Also the theory can be extended to account for the effects of non-negligible electric field strengths.

In their letter, EC calculated the zero-field mobility of electrons in helium gas with densities from 10^{20} atoms/cm^3 to 25×10^{20} atoms/cm^3 at temperatures of 3.65, 3.90, and 4.19 °K. This range of density and temperature allowed comparison with the data of Levine and Sanders.[2] Recently, Harrison and Springett[3] have performed measurements over a substantially larger temperature range. Their data are fairly extensive in the region $4.2 \leq T \leq 18.1$ °K. It is possible to take the theory, without change, and calculate the zero-field mobility over this extended temperature range. It is found that the parameters appropriate to 4 °K are not quite appropriate at higher temperatures, but a fit can be found. The sensitivity of the theory to the parameters will be shown.

Further, using a theory of Cohen and Lekner,[4] suitably modified for this problem, the manifestation of the influence of non-negligible electric fields on the observed drift velocity of electrons can be calculated. A comparison of the results with the field-dependent data of Levine and Sanders[2] shows adequate agreement but emphasizes the fact that,